1   # Comparative studies of CO₂ capture solvents for gas-fired power plants:

2   # Integrated modelling and pilot plant assessments

3   **Sharifzadeh, Mahdi[1a]; Shah, Nilay[a]**

4   [a] Centre for Process Systems Engineering (CPSE), Department of Chemical Engineering, Imperial College. London SW7 2AZ

5

6   **Abstract-** Natural gas accounts for 21.3% of the total primary energy supply. In particular, with the shale gas

7   boom, its application has experienced an exponential growth rate. Nevertheless, natural gas has the highest

8   hydrogen to carbon ratio among all hydrocarbons and the dilute (with respect to CO_2) exhausts of its

9   combustion pose considerable thermodynamic challenges for carbon capture. Solvent-based carbon capture

10   can potentially mitigate the carbon emissions. Nonetheless, minimizing the penalties associated with the costs

11   of carbon capture requires detailed understanding of the underlying physical and chemical phenomena. The

12   present research exploits a rigorous methodology based on rate-based distributed modelling and statistical

13   associating fluid theory (SAFT). The important characteristics of this modelling approach include abstract

14   formulation in conjunction with high predictability. The present research aims at establishing the performance

15   of a new solvent (an amine-promoted buffer salt, APBS) in comparison to the baseline solvent, *i.e.*,

16   monoethanolamine (MEA). The features of interest include: (i) developing a high fidelity mathematical model

17   of the carbon capture process, (ii) validating the model with pilot plant data, (iii) quantification of the energetic

18   and technical performances of the solvents using key process indicators (KPIs), and (iv) employing optimization

19   programming for further solvent performance improvement.

20

21   **Keywords:** Solvent-based carbon capture, SAFT, rate-based modelling, model validation, optimization, MEA,

22   APBS, GCCmax.

23

---

[1] * **Corresponding Author:** Dr Mahdi Sharifzadeh; Room C603, Roderic Hill Building, South Kensington Campus, Imperial College London, UK. SW7 2AZ. E-mail: mahdi@imperial.ac.uk ; Tel: +44(0)7517853422

1.   Introduction

Increasing energy demand and associated pollution have posed an important paradoxical challenge toward the security of energy supply and environmental protection. This has translated into various national and global policies and regulations. The instances of these international regulations include the so-called Europe 2020 which targets 20% reductions in greenhouse gases, 20% energy supply from renewables, and 20% improvement in energy efficiency. In the UK, the Climate Change Act 2008 mandates an 80% overall cut in six greenhouse gases by 2050 compared to the 1990 baseline. While integration of renewable energy resources can moderate the problem to some extent, the Intentional Energy Agency (IEA) asserts that in a foreseeable future, fossil fuels remain the dominant source of energy supply, and application of carbon capture technologies will become increasingly urgent (IEA 2014a).

Natural gas (NG) accounts for 21.3% of the global primary energy supply (IEA 2014b) and with the shale gas boom, its application has experienced an exponential growth rate. Nevertheless, natural gas has the highest hydrogen to carbon ratio among all hydrocarbons and the dilute (with respect to CO_2) exhausts of its combustion pose considerable thermodynamic challenges for carbon capture. Amongst various carbon capture methods, post-combustion has the advantage of being an end-of-pipe treatment, requiring a minimal of retrofit to the existing energy infrastructure. In particular, solvent-based carbon capture has been already applied in ammonia and natural gas sweetening processes and is deemed to be the most commercially viable technology for end-of-pipe waste treatment of power plants. Furthermore, solvent-based carbon capture has proved to be an efficient method for increasing the yield of biorefineries (Sharifzadeh, et al., 2015) and emission reduction in the iron and steel industry (Ho et al., 2013).

In the recent years, developing solvents with superior techno-economic performance has been the focus of academic and industrial researchers. Frimpong et al., (2013) compared the performance of a proprietary amine-carbonate blend for carbon capture from coal-derived flue gas. The comparison with MEA baseline solvent was made based on carbon capture efficiency, energy of solvent regeneration, and overall mass transfer rate. Both solvents were studied at similar experimental conditions. Moser et al., (2011a,b) evaluated the performance of a solvent developed by BASF in a highly instrumented pilot plant in Niederaussem. They used CHEMASIM, an in-house simulation software tool, for data reconciliation and model validation. Their results suggested a high correlation between the reboiler duty, the desorber pressure, solvent circulations

52 rate, and solvent heat of absorption. Similar observation was made by Bumb et al., (2014) who studied the

53 performance of a novel solvent optimized for coal-fired flue gas, at TNO pilot plant, Netherlands. They studied

54 variation of the desorber top pressure between 0.8-1 barg, while maintaining the reboiler temperature

55 constant. They reported that reboiler heating duty and solvent circulation were both minimum at 0.8 barg.

56 However any further reduction would result in unacceptable condensate rate from the desorber overhead.

57 Mangalapally et al., (20111a,b, 2012) conducted pilot plant studies for four new solvents. They identified the

58 solvent circulation rate as the most influential operating parameter for pilot plant operation. Rabensteiner et

59 al., (2014) studied pilot scale performance of ethylenediamine (EDA) compared to MEA using literature data.

60 Cousins et al., (2012, 2015) studied the performance of concentrated piperazine and MEA in an Australian pilot

61 plant. They observed that at elevated liquid/gas ratio, absorber intercoolers can mitigate the regeneration

62 energy requirements by 10%. They also reported that rich solvent split can result in less reboiler and

63 condenser duties.

64 An ideal solvent should have high CO_2 loading, fast reaction kinetics, low vapour pressure, negligible

65 corrosiveness, and high thermal stability, in addition to a lower cost. Often these criteria are interdependent

66 and require establishing a compromise. Oexmann and Kather (2010) provided an analytic analysis of thermal

67 requirements for solvent regeneration heating duty, as a function of (i) solvent sensible heat (energy needed

68 to increase the solvent temperature from absorber temperature to desorber temperature), (2) heat of

69 evaporation (to produced stripping steam in the desorber), and (3) heat of desorption (needed to break the

70 solvent-CO_2 bound). They demonstrated that these solvent characteristics are often interdependent. Solvents

71 with a high heat of absorption often feature a higher kinetic rate. Furthermore, since the desorber can be

72 operated at a higher pressure and the reboiler can be operated as a higher temperature, the water reflux from

73 the desorber overhead is lower; hence the heating duty of the desorber will be also lower. Furthermore, a

74 faster kinetic enables higher CO_2 loading and therefore, resulting in less solvent circulation rate and hence less

75 sensible heat requirement. Nevertheless, the maximum allowable temperature in the desorber depends of the

76 solvent thermal stability against degradation reactions. By comparison solvents with a lower heat of

77 absorption may benefit from operating the desorber in vacuum operating conditions, at the costs of a higher

78 power requirement for CO_2 compression.

79   More recent studies have focused on solvents with additional functionalities. For example, ammonia is

80   regarded as a cost-effective solvent for CO_2 separation. However, low absorption rates limit the practical

81   application of this solvent. Yang et al., (2014) investigated the effects of adding potassium sarcosinate as the

82   rate promoter to the ammonia solvent. Similarly, Thee et al., (2012) showed that the addition of small

83   quantities of MEA to potassium carbonate solvent results in radical increases in the overall reaction rate.

84   Recently, a new class of solvent is introduced, which exploit phase change in order to limit the energetic

85   penalties of solvent regeneration. For example as shown by Liebenthal et al., (2013), an amine blend can form

86   two liquid phases under certain CO_2 loading conditions. Then, a large energy saving is possible by sending only

87   the CO_2-rich phase to the desorber. Furthermore, Ionic liquids are a promising class of solvents for carbon

88   capture. The tunability of the ionic liquids' structure and properties offers several advantages such as lower

89   energy requirement for solvent regeneration, higher thermal stability, and lower vapour pressure. However,

90   the high production cost of ionic liquids is a barrier that needs to be addressed for their commercialization,

91   (Chen et al., 2014).

92   Finally, process optimization has been the focus of various studies. Lee et al., (2013) investigated the

93   performance of several amine solvents. They demonstrated a strong trade-off between the capital investment

94   and operating costs using Pareto front diagrams. Mores et al., (2012) studied simultaneous optimization of the

95   dimensions of the process equipment and process operating conditions. Three scenarios were considered in

96   which reboiler duty was being optimized with respect to different combinations of reboiler inlet liquid flow-

97   rate, reboiler inlet solvent composition, reboiler pressure, CO_2 loading and CO_2 recovery target. They observed

98   a correlation between the optimal solvent CO_2 loading and the CO_2 recovery targets. In addition, they reported

99   that as CO_2 loading increases, the specific heating and cooling duties (per unit of CO2 recovered) decrease.

100 Hopkinson et al., (2014) developed a simple method for optimization of a conceptual solvent based on

101 properties of commercial amine solvents. Solvent heat of reaction was applied in order to estimate the

102 sensible and stripping heat of the process. They reported the value of 71 kJ/mol CO2 for the heat of reaction

103 and the value of 0.1034 kWh/kg CO2 for the total equivalent work in the case of 90% CO2 recovery from coal-

104 fired flue gases. Damartzis et al., (2015) proposed a module-based generalized design framework in order to

105 synthesize the optimal process flow diagram. Features of interest included the stream topologies, the heat

106 redistribution and the cascades of desorption columns for several commercially available solvents. Significant

107 economic improvement (15%-35%) and reductions in the reboiler duty (up to 55%) were observed. Recently,

108 Burger et al., (2015) proposed a hierarchical methodology based on a group contribution method which

109 considers the molecular decisions at the same level of process design decisions. They demonstrated their

110 method for selection of the optimal solvent over a wide range of ethers, for CO_2 separation from a methane-

111 rich mixture.

112 Several common conclusions can be drawn from the aforementioned theoretical and pilot plant studies.

113 - In establishing the performance of new solvents, there is always a need for a well-understood and

114 predictable reference solvent such as monoethanolamine (MEA) which facilitates pilot plant testing

115 runs and provides benchmark performance measures.

116 - Due to interdependencies of process operating specifications and combinatorial characteristics of the

117 involved parameters, the pilot plant studies were often conducted in conjunction with simulation and

118 optimization software tools.

119 - The pilot plant operating conditions are solvent-specific and the performance of each solvent should

120 be studied at its corresponding optimal specifications.

121 - There is a need for key performance indicators which are not solvent-specific and are reproducible for

122 different solvents.

123 The present research aims at benchmarking the performance of a new solvent called GCCmax. The GCCmax

124 solvent is a novel solvent recently developed by Carbon Clean Solutions Limited (CCSL) for carbon capture from

125 natural gas combustion exhausts and belongs to the class of amine-promoted buffer salt (APBS) solvents. The

126 conducted research is comprehensive and include, pilot plant studies, model development and validation, and

127 optimization in order to provide guidelines for further solvent optimization. The novel contribution of the

128 present research includes:

129 1. Developing high fidelity multi-scale models for post-combustion carbon capture and validating the

130 model for the case of the GCCmax and MEA solvents using pilot plant data.

131 2. Quantification of the performance of the solvents using a novel set of key performance indicators

132 (KPIs), that enables objective and reproducible comparisons.

133 3. Identification of further opportunities for process optimization in terms of equipment design,

134 operating conditions, and solvent composition.

135 The rest of the manuscript is organized as follows. Firstly, the research methodology is discussed. The features

136 of interest include the applied modelling approach and underlying assumptions. Then, the results of model

137 validation are presented and compared for the baseline MEA solvent and the new GCCmax solvent. The

138 comparison is made based on several novel key process indicators which quantify the difficulty of separating

139 CO_2 from the flue gas. These "technical" KPIs are used as substitutes for economic indicators because using the

140 latter to compare alternative solvents would suffer from assumptions around the cost of capital, the capital

141 estimation method and the cost of utilities, limiting the reproducibility of the results. The last part of the paper

142 explores the opportunities for further improvement of the new solvent performance through optimization

143 with respect to process equipment, operating conditions, and the solvent composition.

144 **2. Methodology**

145 The research methodology is based on a multi-scale process modelling and optimization. Firstly, a rigorous

146 process model was developed based on accurate understanding of the involved physical and chemical

147 phenomena and rate-based modelling of gas-liquid contactors. Then, the developed model is validated using

148 pilot plant data. Finally, the validated model is optimized for various design and retrofit scenarios.

149 **2.1. Process model development**

150 The accurate modelling of the solvent-based CO_2 capture processes for the purposes of solvent benchmarking

151 and comparison requires thorough understanding of the underlying physical and chemical phenomena

152 involved in absorption and desorption of CO_2 into and from the working solvent. The methods for modelling

153 gas-liquid contactors can be broadly classified into equilibrium and rate-based models. Early-stage attempts

154 for modelling gas-liquid separation processes were based on the assumption that at each separation stage, the

155 exiting phases are in equilibrium conditions. Such assumptions were also incorporated into graphical methods

156 (McCabe et al., 2004). However, it was widely observed that for most industrial applications assuming

157 equilibrium composition of the exiting phases results in unrealistic predictions. The first attempt to overcome

158 this limitation was to consider an efficiency measure for each separation stage, (McCabe et al., 2004), which

159 can be applied to calculate the actual number of stages from the theoretical number of stages. Application of

160 empirical efficiency correlations has been promising for binary and close-boiling separation systems. However,

161 it was widely observed that for multicomponent systems, the efficiency of separation stages can vary from 5%

162 for absorption systems with high viscosity, high molecular weight solvents to 120% in single-liquid-pass large-

163   diameter distillation trays (or packed segments) because of the crossflow effect (Seader et al., 2013). Due to

164   difficulties associated with uncertainties in the stage efficiency method, intensive research was devoted to

165   developing non-equilibrium models based on transport rates (Waggoner and Loud, 1977; Krishna and Standart

166   1979; Taylor and Krishna, 1993; Krishnamurthy and Taylor, 1985; Taylor et al., 1994). The rate-based models

167   are founded on the two-film theory, as shown in Fig. 1. Here, thermodynamic equilibrium is assumed only at

168   the interface of vapour and liquid phases. Unlike equilibrium-based models, the exiting vapour phase is

169   superheated and the exiting liquid phase is subcooled and they have different temperatures. The exchanged

170   mass and energy between phases depend on the driving forces, transport coefficients, and the interfacial area.

171   Often, both convective and diffusive transport phenomena are involved and component-coupling effects

172   should be considered (Seader et al., 2013). Various empirical correlations for calculating the mass transfer

173   coefficient are proposed by researchers for random packing (Onda et al., 1968; Bravo and Fair, 1982) and

174   structured packing (Bravo et al., 1985, 1992). Finally, the bulk liquid and gas phases may have different flow

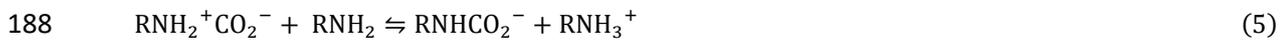175   configurations such as plug or mixed flows.
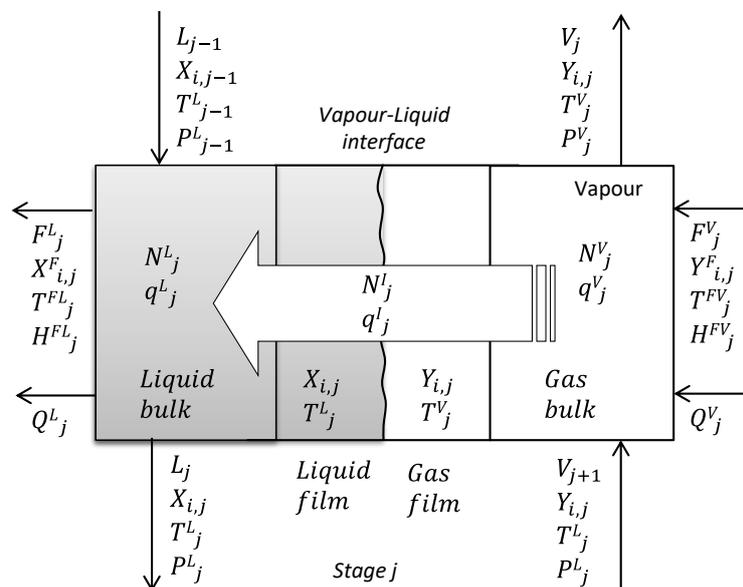
176

177   Fig. 1. Two-film model used for modelling rate-based absorption and desorption of CO_2 into and from solvent,

178   (Zhang et al., 2009).

179   ## 2.2.   Reaction kinetics and thermodynamics

180   A full space rate-based representation of CO_2-solvent gas-liquid contactors requires detailed modelling of

181   underlying chemical reactions, column hydraulics, as well as mass and heat transfer phenomena. For the case

182   of CO_2 capture using alkanolamines, this would require modelling a series of speciation reactions as follows

183   (Mac Dowell et al., 2010):

184    $$2H_2O \leftrightharpoons H_3O^+ + OH^- \tag{1}$$

185    $$CO_2 + H_2O \leftrightharpoons HCO_3^- + H^+ \tag{2}$$

186    $$CO_2 + OH^- \leftrightharpoons HCO_3^- \tag{3}$$

187    $$CO_2 + RNH_2 \leftrightharpoons RNH_2^+CO_2^- \tag{4}$$

188    $$RNH_2^+CO_2^- + RNH_2 \leftrightharpoons RNHCO_2^- + RNH_3^+ \tag{5}$$

189    $$RNHCO_2^- + H_2O \leftrightharpoons RNH_2 + HCO_3^- \tag{6}$$

190   where for the case of MEA, R=HO-CH2-CH2- . In the scheme above, reaction (1) represents water hydrolysis,

191   reactions (2) and (3) are concerned with carbonic acid and bicarbonate formation, respectively. Reaction (4)

192   represents the Zwitterion formation and reaction (5) is base catalysis. The two latter reactions are highly

193   coupled as carbamate and protonated amines are tightly bonded. Therefore, reaction (4) and (5) can be shown

194   abstractly as:

195    $$CO_2 + 2RNH_2 \leftrightharpoons [RNHCO_2^- + RNH_3^+] \tag{7}$$

196   Reaction (7) is a reversible acid-base neutralization reaction. In this reaction, absorption of CO_2 in

197   alkanolamine solvent is exothermic; hence, it is possible to liberate CO_2 by heating the CO_2-rich solvent

198   mixture and driving the reaction to left. Therefore, in theory, it is possible to regenerate the alkanolamine and

199   recycle it for reuse in the absorber. In practice, a small amount solvent make-up is supplied to compensate the

200   losses associated with the solvent escape and degradation reactions.

201   Various thermodynamic models were proposed by researchers in order to describe the thermophysical

202   properties of the mixture of CO_2 absorbed into alkanolamines. These methods can be broadly categorized to

203   non-rigorous and rigorous methods. In non-rigorous methods, equilibrium constants are considered for the

204   aforementioned reactions and are reconciled against experimental data. The major drawback of non-rigorous

205   methods is the lack of precision for closing energy balances and predicting speciation of components [17]. In

206   addition, the rigorous methods can be classified to (1) activity-based models (derived from Gibbs free energy),

207   and (2) equation of state models (derived from Helmholtz free energy). A frequently used activity-based model

208   is Electrolyte Non-random two-liquid model (E-NRTL) in which the activity coefficient expressions of the

209   original NRTL model are modified, and certain constraints regarding local like-ion repulsion and

210   electroneutrality are imposed (Chen and Song, 2004). An alternative activity based model is the Extended

211   UNIQUAC model where the original UNIQUAC model was modified to account for ionic interactions (Faramarzi

212   et al., 2009). A limitation of the aforementioned activity-based models is that they only describe the liquid

213   phase and a separate equation of state (e.g., Soave–Redlich–Kwong equation of state by Faramarzi et al.,

214   2009) should be applied for modelling the vapour phase. Alternatively, researchers attempted to use

215   equations of states which can consider the presence of ionic components (Huttenhuis et al., 2008). More

216   recently, application of equations of state which are able to accommodate chemical equilibria such as

217   association between molecules, has been the focus of various research groups (Fürst and Renon, 1993; Button

218   and Gubbins, 1999). Here, the treatment is based on statistical associating fluid theory (SAFT), in which the

219   free Helmholtz energy is correlated to the intermolecular association between the molecule segments

220   (Chapman et al., 1989; Mac Dowell et al., 2010):

221
$$\frac{A^{mix}}{NkT} = \frac{A^{IDEAL}}{NkT} + \frac{A^{MONO}}{NkT} + \frac{A^{CHAIN}}{NkT} + \frac{A^{ASSOC}}{NkT} \tag{8}$$

222   In above, N refers to the number of molecules, k is the Boltzmann constant and T is the mixture temperature.

223   On the right-hand-side, the first term represents the ideal Helmholtz free energy and the three other terms

224   refer to the residual contribution due to monomers interactions, formation of chains, and intermolecular

225   interaction between associating sites. Then, given the Helmholtz free energy of the mixture, A^{mix}, it is possible

226   to calculate other mixture properties (e.g., $\mu_i = (\delta A / \delta N_i)_{T,V,N_{i \neq j}}$). The association contribution is based on

227   thermodynamic perturbation theory (TPT) (Wertheim, 1984), where by using intermolecular potential models

228   (e.g., square well with variable range) and by adjusting their parameters (well depth and range), it is possible

229   to fully characterize the strength of the associating sites.
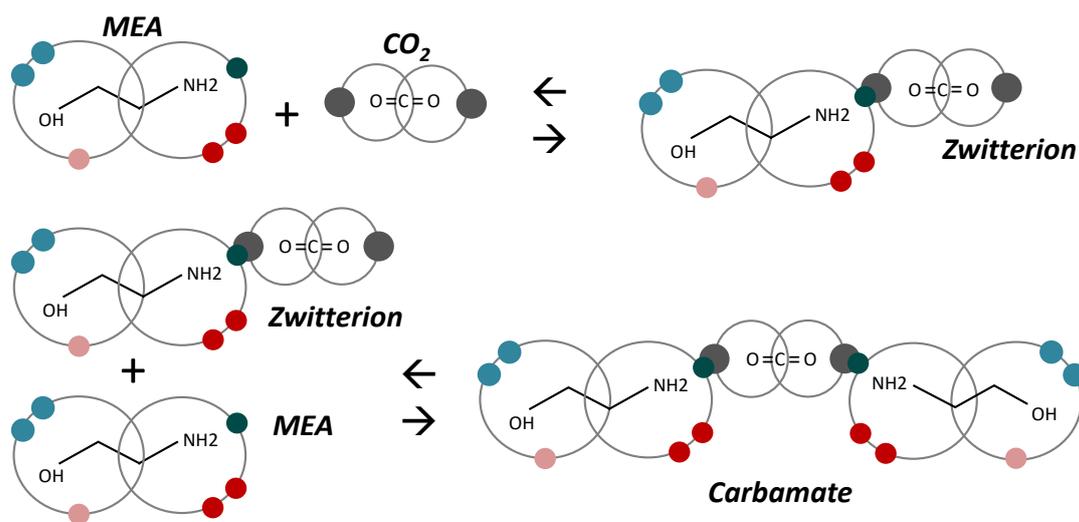
230

231 **Fig. 2. Schematic representation of Carbamate formation**

232 The idea is shown in Fig. 2 for the case of reaction (4) and (5), (Mac Dowell et al., 2010). In the new approach,

233 the rate of reactions, the concentration of intermediate zwitterion, and its thermophysical properties are not

234 formulated anymore. Instead, CO_2 and MEA are represented as associating molecule chains with two and six

235 associating sites, respectively. Then, the concentration of CO_2 in association with two MEA molecules

236 represents the actual CO_2 loading of the solvent at different temperatures and pressures. The combination of

237 rate-based modelling and representation of chemical reactions using statistical associating fluid theory (SAFT)

238 provides a consistent modelling approach. The justification is that for solvents such as MEA and GCCmax, the

239 rate of reaction is significantly faster than the heat and mass transfer phenomena. Therefore, the knowledge

240 of the rate of reactions at the gas-liquid interface is unnecessary and the chemical equilibrium sufficiently

241 describes the actual physical system behaviour. It is notable that in the case of solvents for which the reaction

242 kinetics are not fast enough, this modelling approach may introduce approximations.

243 This modelling approach offers several advantages; firstly unlike activity-based models, the same equation of

244 state is used to describe both liquid and vapour phases. Secondly, the chemical equilibria are treated at the

245 same level as phase equilibria. Furthermore, this approach results in significant model reduction because the

246 speciation of intermediate ions is not included in the mathematical formulation and the uncertainties

247 associated with their thermophysical parameters are disentangled from problem formulation. Most of all, the

248 aforementioned approach establishes a connection between the chemical and physical behaviour of the

249 mixture and the molecular structure of the involved materials. This is of particular importance to new solvents

250   as the required information can be acquired from the available data for the molecular segments of associating

251   sites from literature experimental data.

252   In the present research, rate-based gas-liquid contactors were developed based on a combination of two-film

253   theory and statistical associating fluid theory for potentials of variable range (SAFT-VR). The applied software

254   tools were advanced modelling library gas-liquid contactors (AML-GLC) and gSAFT toolboxes developed by

255   Process System Enterprise Ltd (PSE). The parametric values of thermodynamic models for the GCCmax solvent

256   are obscured in order to respect the confidentiality agreements with Carbon Clean Solutions Limited (CCSL)

257   and Process System Enterprise (PSE). The underlying mathematical modelling of the gas-liquid contactors were

258   similar to (MacDowell et al., 2013). The SAFT thermodynamic model and its application for modelling CO_2

259   capture solvent are described by MacDowell et al., (2010).

3. Pilot plant operation and model validation

261   In order to ensure effective benchmarking and model validation, two sets of pilot plant runs were conducted

262   using the monoethanolamine (MEA) and GCCmax solvents. MEA served as the baseline reference solvent. The

263   pilot plant studies were conducted in the US National Carbon Capture Center (NCCC) located in Alabama, USA.

264   The capture process is shown in Fig. 3, which is based on a more detailed process flow diagram in (Gayheart et

265   al., 2013). The column specifications for the capture process in the National Carbon Capture Center (NCCC) are

266   reported in Table 1. The process description is as follows. Firstly, the pressure of the pre-scrubbed and cooled

267   flue gas is increased via a blower and then is sent to the absorber column. In the absorber column, flue gas is

268   brought in contact with the lean solvent, and the CO_2 is chemisorbed into the solvent. The absorption process

269   is exothermic and the released heat increases the solvent temperature. The solvent enriched with the

270   absorbed CO_2 is sent to the desorber column where the carbon dioxide is released through heating. Before,

271   recycling the hot lean solvent to the absorber column for reuse, there is an opportunity for heat integration to

272   the rich solvent. Additional cooling will be provided using cooling water. The solvent and water losses are

273   compensated with adequate make-ups.

274   **Table 1. Column Specifications (Gayheart et al., 2013).**

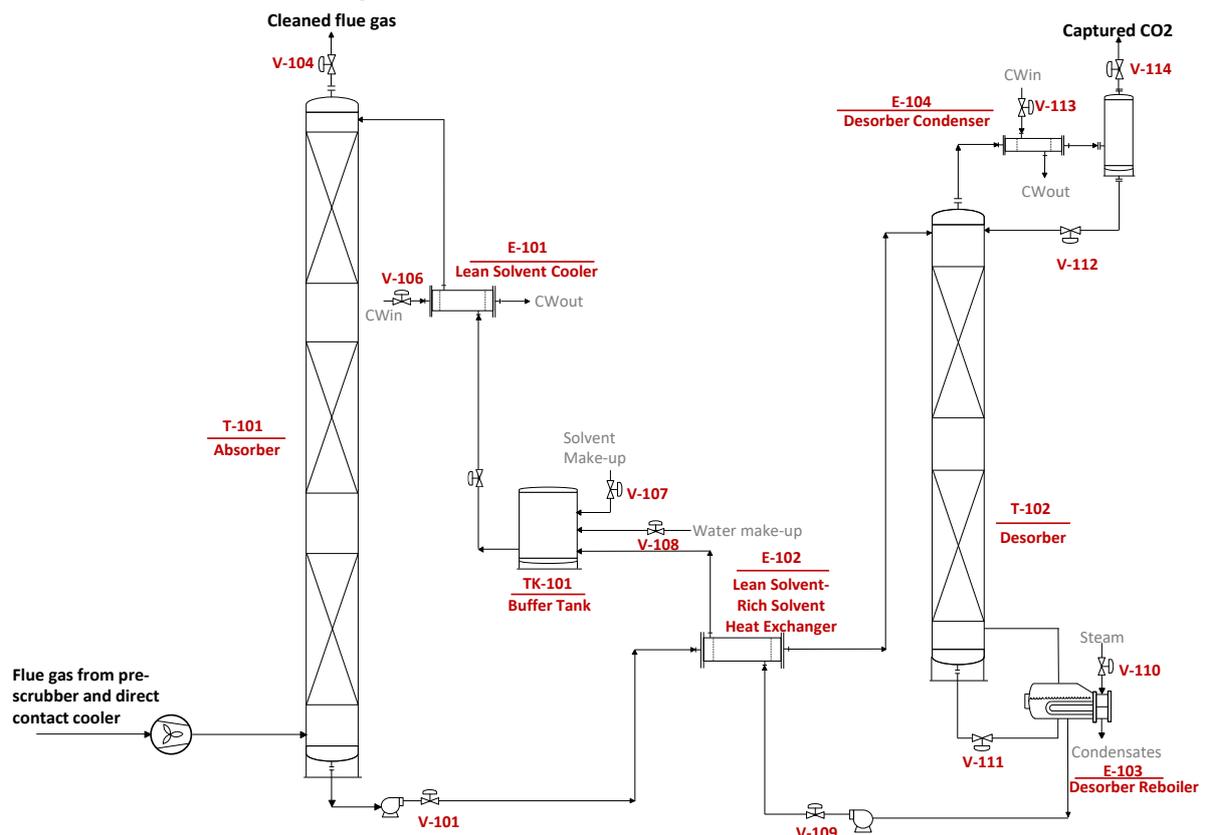| Column	Packing	Height of each bed (m)	Diameter (m)	Number of beds
Absorber	Mellapakplus M252Y- Steel	6.1	0.66	3
Desorber	Mellapakplus M252Y- Steel	6.1	0.61	2

275

276
277 **Fig. 3. A representative flow diagram of the US Natural Carbon Capture Center (NCCC) CO₂ capture pilot**

278 **plant, Alabama, US (Gayheart et al., 2013).**

279 Table 2 shows the results of model validation. Since the NCCC pilot plant was not previously operated under

280 natural gas exhaust conditions, the model validation was conducted based on historical data for a scenario of

281 coal-fired exhausts. The last column in Table 2 reports the prediction of the model, when the process is

282 operated under natural gas exhaust conditions. Table 2 shows a very good agreement between pilot plant data

283 and simulation results, in terms of captured CO_2, and the solvent composition. Minor discrepancies in the

284 consumed steam are deemed to be associated with heat losses and temperature indicator errors. Table 3

285 reports the results of the GCCmax solvent model validation under natural-gas-fired conditions. Two sets of

286 pilot plant data were used, which essentially are different with respect to the lean solvent temperature

287 entering the absorber top. The justification was due to the fact that in different parts of the world, cooling

288 water may be supplied at different temperatures. Again the model predictions are in very good agreement

289 with the pilot plant data with respect to the captured CO_2 and the solvent concentrations, giving confidence in

290 the model's predictive capabilities. Minor discrepancies in the required steam and temperatures were

291 attributed to lack of insulation or temperature measurement errors.

292

293

294   **Table 2. Model validation for MEA baseline solvent.**

		Alabama-coal	Alabama-coal	Alabama NG
		Pilot Plant	Simulation	Simulation
Flue gas to the absorber				
Nitrogen + Oxygen	Mass Fraction	0.786	0.786	0.909
Carbon Dioxide	Mass Fraction	0.165	0.165	0.067
Water	Mass Fraction	0.049	0.049	0.024
Total flowrate	kg/s	0.628	0.628	0.628
Flue Gas Temperature - Absorber Inlet	K	316.56	316.56	316.56
Lean Solvent - Absorber Inlet				
Amine	Mass Fraction	0.297	0.298	0.296
CO_2	Mass Fraction	0.063	0.059	0.059
Water	Mass Fraction	0.640	0.643	0.645
Total	kg/s	2.52	2.51	1.3
Lean solvent temperature	K	316.15	316.15	316.15
Intercoolers outlet temperature	K	316.15	316.15	-
Reboiler Steam				
Steam pressure	bar	2.92	2.92	2.92
Steam temperature	K	405.6	405.6	405.6
Steam flowrate	kg/s	0.18	0.15	0.07
Lean-Rich Heat Exchanger				
Lean in	K	388.87	388.9	389
Lean out	K	331.4	338.9	330.8
Rich in	K	327.91	330.4	321.7
Reboiler temperature	K	385.6	388.0	389.0
Absorber bottom pressure	bar	1.1	1.17	1.16
Absorber top pressure	bar	1.04	1.04	1.04
Desorber bottom (reboiler) pressure	bar	1.71	1.71	1.16
Desorber top pressure	bar	1.69	1.70	1.70
General specifications				
CO_2 capture efficiency	%	91.84	91.85	90
Inter-stage Cooling		Yes	Yes	No

295

296 **Table 3. Model validation for GCCmax solvent.**

		Data Set 1	Data Set 1	Data Set 2	Data Set 2
		Pilot Plant	Simulation	Pilot Plant	Simulation
Absorber inlet gas stream					
Nitrogen + Oxygen	Mass Fraction	0.895	0.895	0.896	0.896
Carbon dioxide	Mass Fraction	0.065	0.065	0.065	0.065
Water	Mass Fraction	0.040	0.040	0.039	0.039
Temperature	K	313.1	313.1	312.8	312.8
Total flowrate	kg/s	0.995	0.995	0.9951	0.9951
Absorber					
Absorber top pressure	bara	1.160	1.160	1.160	1.160
Absorber bottom pressure	bara	unavailable	1.224	unavailable	1.221
Absorber outlet CO_2 concentration	Mass Fraction	0.0053	0.0056	0.004	0.005
Lean solvent - absorber inlet temperature	K	304.1	304.1	325.4	325.4
Rich solvent - absorber outlet temperature	K	318.1	316.5	318.7	316.1
Lean solvent flowrate	kg/s	0.857	0.857	0.756	0.756
Desorber (regenerator)					
Desorber Bottom Temperature	K	388.6	388.6	395.4	395
Desorber Top Pressure	bara	1.701	1.708	2.031	2.03
CO_2 stream	kg/s	0.0578	0.0611	0.060	0.0605
Reboiler Steam					
Steam pressure	bar	3.606	3.605	4.075	4.075
Steam temperature	K	402.8	402.8	408.5	408.5
Steam condensate Temperature	K	401.9	401.9	407.8	407.5
Steam flowrate	kg/s	0.091	0.078	0.086	0.0823
Lean-Rich Heat Exchanger Temperatures					
Lean solvent in	K	387.4	388.6	394.2	395.0
Lean solvent out	K	325.0	322.6	324.7	327.4
Rich solvent in	K	318.9	316.5	319.9	316.1
Rich solvent out	K	380.4	379.9	384.0	379.9
Lean solvent concentration					
GCCmax Solvent	Mass Fraction	0.410	0.410	0.439	0.439
Water	Mass Fraction	0.536	0.541	0.504	0.515
CO_2	Mass Fraction	0.054	0.049	0.057	0.046
General specifications					
CO_2 Capture Efficiency	%	89.1	91.7	92.50	92.13
Inter-stage Cooling		No	No	No	No

297
298

299 The validated pilot plant model was used to extract several technical key process indicators (KPIs) which are

300 important measures that quantify the difficulties associated with CO_2 separation from the flue gas in terms of

301 the required heating and cooling duties, required packing, and solvent circulation. These measures are scaled

302 with respect to the amount of pure CO_2 captured, to become independent of the pilot plant throughput and

303 enable comparisons. Table 4 provides the comparisons between the solvents. This table reveals that compared

304 to the MEA reference solvent, the GCCmax solvent requires 25.4-29.4% less steam for solvent regeneration in

305 the reboiler, per ton of CO_2. In addition, compared to the MEA reference solvent, the GCCmax solvent requires

306 73-84.4% less cooling water in the condenser and intercooler. The volume of packing in the absorber and

307 desorber columns also shows improvements in the case of the GCCmax solvent. Finally, the GCCmax solvent

308 circulation is 58.8-64.7% less than MEA solvent circulation which implies significant reductions in the electricity

309 power needed for solvent pumping.

310 **Table 4. Key process indicators (KPIs) for the GCCmax solvent and baseline MEA solvent**

Key Process Indicators (KPIs)	Unit	MEA	GCCmax (Data1)	GCCmax (Data2)
Heating duty	(MJ/ton CO_2)	3986	2813	2975
Cooling duty	(MJ/ton CO_2)	5644	1524	884
Volume of packing	(m3/ton CO_2 hr-1)	46.619	45.64	45.91
Solvent circulation flow rate	(ton solvent/ton CO_2)	34	14	12

311

4. Solvent performance optimization

313 The last part of the present research was concerned with model-based optimization of the carbon capture

314 process. Having validated the process model using pilot plant data, we wished to explore the improvement

315 opportunities and the significance of various investment and operational decisions. Three scenarios were

316 studied:

317 In Scenario (1), the dimensions of process equipment and operating conditions were optimized

318 simultaneously. This scenario represents the case where the plant is built for the first time.

319 In Scenario (2), the dimensions of process equipment are fixed and only the operating conditions are

320 optimized. This study is concerned with the scenario where an existing process is adapted to a new

321 solvent.

322   In Scenario (3), similar to the second scenario, the dimensions of process equipment are fixed. However,

323   operating conditions and the GCCmax solvent blend composition are optimized simultaneously. This

324   scenario highlights the implication of the solvent optimization for energy saving.

325   In the first scenario, the objective function was the Total Annualized Costs because:

326
$$Total\ Annualized\ Costs = \frac{Fixed\ Capital\ investment}{Plant\ effective\ Life} + Total\ Annual\ Energy\ costs \qquad (9)$$

327   However, since in the second and third scenarios the equipment dimensions are fixed, the first right-hand-side

328   term of the above equation is constant and only Total Annual Energy Costs are optimized. In equation (9), the

329   value of 5 years were considered for the plant life cycle, in order to incorporate interest rate and the time

330   value of money. The costs of process equipment were calculated according to the costing correlations

331   provided in (Couper et al., 2012). Lang factor of 6 was considered for estimating the total capital investment

332   (Peters et al., 2004). The considered utility costs were 37.02 $/MWh for electricity (Electricity Wholesale

333   Market 2015), 0.048 $/tonne for cooling water (Ulrich and Vasudevan, 2006), and 14.5 $/tonne for steam. Two

334   additional constraints were considered:

335    $Carbon\ capture\ = 90\%$ $\qquad\qquad\qquad\qquad\qquad\qquad\qquad\qquad\qquad\qquad\qquad (10)$

336    $Reboiler\ temperature < \ 120\ ^oC$ $\qquad\qquad\qquad\qquad\qquad\qquad\qquad\qquad\qquad (11)$

337   The first constraint ensures that 90% CO_2 is captured from the flue gas. The second constraint limits the

338   maximum reboiler temperature in order to avoid solvent degradation. Table 5 presents the results of

339   optimization. A comparison between Scenario (1) in which process equipment was being optimized and the

340   other two scenarios, suggests that the size of the pilot-plant absorber and desorber columns was larger than

341   the required values. This is an intuitive observation, because pilot plants are often to an extent overdesigned

342   in order to allow a variety of solvent testing. In the first scenario, the heating and cooling duties are slightly

343   higher than the other two scenarios, as they were optimized in conjunction with capital investment. In the

344   other two scenarios, the process equipment items were fixed and the optimizer took the opportunity to

345   exploit process equipment for energy saving. It is notable that there is a significant energy saving when the

346   solvent composition and operating conditions were optimized simultaneously, which illustrates the

347   importance of solvent control and optimization during process operation.

348

349 **Table 5. Optimization results**

		Scenario (1)	Scenario (2)	Scenario (3)
Optimization objective function		Total annualized costs	Annualized energy costs	Annualized energy costs
Optimization variables		*Equipment size and operating conditions*	*Operating conditions only*	*Operating conditions and solvent composition*
Flue gas to absorber				
H2O	mass fraction	0.0388	0.0388	0.0388
CO$_2$	mass fraction	0.0651	0.0651	0.0651
N2	mass fraction	0.7320	0.7320	0.7320
O2	mass fraction	0.1640	0.1640	0.1640
Pressure	Pa	1.22E+05	1.22E+05	1.22E+05
Temperature	K	312.8	312.8	312.8
Flowrate	kg/s	0.995	0.995	0.995
Absorber diameter	m	0.5	0.66	0.66
Absorber height	m	9	18.3	18.3
Lean Solvent to absorber				
Flowrate	kg/s	0.787	0.874	0.739
Temperature	K	324.2	319.9	320.2
Composition				
H2O	mass fraction	0.5390	0.5390	0.5470
CO$_2$	mass fraction	0.0517	0.0517	0.0444
GCCmax	mass fraction	0.4093	0.4093	0.4086*
Reboiler temperature	K	398	398	398
Reboiler steam pressure	Pa	4.07E+05	4.07E+05	4.07E+05
Reboiler steam temperature	K	408.5	408.5	408.5
Reboiler Steam flowrate	kg/s	8.325E-2	7.22E-02	6.282E-2
Lean-Rich heat exchanger				
Lean in	K	398	398.0	398.0
Lean out	K	325.3	321.0	321.2
Rich in	K	317.6	316.3	317.2
Rich out	K	386.7	390.0	390.0
Condenser temperature	K	301.3	301.3	301.5
Desorber condenser duty	W	58909.5	49195.7	43096.1
Lean solvent cooler duty	W	2152.89	2374.1	1936.87
The total cooling duty	W	**61062.39**	**51569.8**	**45032.97**
The heating (Reboiler) duty	W	**176845**	**152554**	**132781**
CO$_2$ Capture		90%	90%	90%

350
351 * The mass fractions of the ingredients of the GCCmax solvent were optimized, with a variation of over 50% in some mass fractions.

352 **5. Conclusions**

353 This paper presented integrated modelling and pilot plant studies in order to benchmark alternative carbon

354 capture solvents, along with key performance indicators (KPIs) to support comparison. The proposed

355 methodology was used to study the technical and energetic performances of GCCmax, a new amine-promoted

356 buffer salt (APBS) solvent, developed by Carbon Clean Solutions Limited (CCSL). In order to obtain meaningful

357 results, a high fidelity model was developed based on rate-based modelling of absorption and desorption

358 columns, in addition to modelling thermodynamic and reaction phenomena based on statistical associating

359 fluid theory (SAFT). The developed model was validated using pilot plant data, with very good agreements

360 between predicted and reconciled data. Detailed comparisons were made based on several key process

361 indicators which quantify the difficulties associated with CO_2 capture and include: the required heating duty,

362 cooling duties, volume of column packing and the solvent circulation rate. The comparisons between key

363 process indicators (KPIs) established the superior performance of the new GCCmax solvent in comparison with

364 the MEA baseline solvent. The last part of this paper explored the opportunities for further improvement of

365 the solvent performance via optimization. The studied scenarios were comprehensive and included (1)

366 designing a new process, (2) retrofitting an existing process using a new solvent and (3) optimizing the solvent

367 composition and the operating conditions of an existing process. While the presented methods are applied for

368 the new GCCmax solvent and the MEA reference solvent, the research methodology is general in nature and

369 can provide an effective standard for solvent comparisons.

370 The present research illustrated the application modelling and pilot plant studies for optimization of the

371 solvent performance. In the future studies, we will apply the developed model for scale up and power plant

372 integration based on the methodology of integrated process design and control (Sharifzadeh 2013a) using

373 inversely controlled process models (Sharifzadeh 2013b; Sharifzadeh and Thornhill 2012, 2013).

374 **Acknowledgements**

378 **References**

379 Billet, R., Schultes, M., 1993. Predicting mass transfer in packed columns. Chem. Eng. Technol., 16, 1–9.

380   Bravo, J. L., Rocha, J. A., Fair, J. R., 1985. Mass transfer in Gauze Packings. Hydrocarbon Processing, 64, 56-60.

381   Bravo, J. L., Rocha, J. A., Fair, J. R., 1992. A comprehensive model for the performance of columns containing

382   structured packings. Inst. Chem. Eng. Symp. Ser., 128 (Distillation and Absorption '92, Vol. 1): A489-A507.

383   Bravo, J.L., Fair, J.R., 1982. Generalized correlation for mass transfer in packed distillation columns. Ind. Eng.

384   Chem. Process Des. Devel., 21, 162–170.

385   Bumb, P., Kumar, R., Khakharia, P., Goetheer, E., 2014. Demonstration of advanced APBS solvent at TNO's CO2

386   capture pilot plant, Energy Procedia, 63, 1657-666.

387   Burger J., Papaioannou V., Gopinath S., Jackson G., Galindo A., Adjiman C.S., 2015. A hierarchical method to

388   integrated solvent and process design of physical CO_2 absorption using the SAFT-γ Mie approach. AIChE

389   Journal, 61 (10), 3249–3269.

390   Button, J. K., Gubbins, K. E., 1999. SAFT prediction of vapour-liquid equilibria of mixtures containing carbon

391   dioxide and aqueous monoethanolamine or diethanolamine. Fluid Phase Equilibria, 158–160, 175-181.

392   Chapman, W. G., Gubbins, K. E., Jackson, G., Radosz, M., 1989. SAFT: Equation-of-state solution model for

393   associating fluids. Fluid Phase Equilib, 52, 31–38.

394   Chen, C.C., Song, Y., 2004. Generalized electrolyte NRTL model for mixed solvent electrolyte systems. AIChE J,

395   50 (8), 1928–1941.

396   Chen, L., Sharifzadeh, M., Mac Dowell, N., Welton, T., Shah, N., Hallett, J.P., 2014. Inexpensive ionic

397   liquids:[HSO 4] -based solvent production at bulk scale, Green Chemistry, 16 (6), 3098-3106.

398   Couper, J.R., Penney, W.R., Fair, J.R., 2012. Chemical Process Equipment Selection and Design (3rd edition),

399   Burlington: Elsevier Science.

400   Cousins, A., Cottrell, A., Lawson, A., Huang, S., Feron, P.H.M., 2012. Model verification and evaluation of the

401   rich-split process modification at an Australian-based post combustion CO2 capture pilot plant.

402   Greenhouse Gas Sci. Technol., 2 (5), 329–345.

403   Cousins, A., Huang, S., Cottrell, A., Feron, P.H.M., Chen, E., Rochelle, G.T., 2015. Pilot-scale parametric

404   evaluation of concentrated piperazine for CO 2 capture at an Australian coal-fi red power station.

405   Greenhouse Gas Sci. Technol., 5, 7–16.

406   Damartzis, T., Papadopoulos, A.I., Seferlis, P. 2015, Process flowsheet design optimization for various amine-

407   based solvents in post-combustion CO2 capture plants. Journal of Cleaner Production. In press.

408   (doi:10.1016/j.jclepro.2015.04.129).

409   Electricity Wholesale Market, [Internet]. Washington: US Energy Information Administration; US Department

410   of Energy c2001-15 [cited 2015 April 8]. Available from: http://www.eia.gov/electricity/wholesale/

411   Faramarzi, L., Kontogeorgis, G.M., Thomsen, K., Stenby, E.H., 2009. Extended UNIQUAC model for

412   thermodynamic modeling of CO2 absorption in aqueous alkanolamine solutions. Fluid Phase Equilib, 282,

413   121–132.

414   Frimpong, R.A., Johnson, D., Richburg, L., Hogston, B., Remias, J.E., Neathery, J.K., Liu, K., 2013. Comparison of

415   solvent performance for CO2 capture from coal-derived flue gas: A pilot scale study. Chem. Eng. Res.

416   Des., 91, 963–969.

417   Fürst, W., Renon, H., 1993. Representation of excess properties of electrolyte solutions using a new equation

418   of state. AIChE J., 39, 335–343.

419   Gayheart, J.W., Moorman, S. A., Parsons, T.R., Poling, C.W., 2013. Babcock & Wilcox Power Generation Group,

420   Inc. RSATTM Process and Field Demonstration of the OptiCapTM Advanced Solvent at the US National

421   Carbon Capture Center. Energy Procedia, 37, 1951–1967.

422   Huttenhuis, P., Agrawal, N., Solbraa, E., Versteeg, G., 2008.The solubility of carbon dioxide in aqueous n-

423   methyldiethanolamine solutions. Fluid Phase Equilib., 264 (1-2), 99–112.

424   Ho, M.T., Bustamante, A., Wiley, D.E., 2013. Comparison of CO2 capture economics for iron and steel mills.

425   International Journal of Greenhouse Gas Control, 19, 145–159.

426   Hopkinson, D., Luebke D., Li Z., Chen S., 2014. Solvent Optimization of Conventional Absorption Processes for

427   CO2 Capture from Postcombustion Flue Gases. Ind. Eng. Chem. Res., 53, 7149−7156.

428   IEA, 2014a. Key World Energy Statistics, International Energy Agency, Paris, France.

429   IEA, 2014b. World Energy Outlook, International Energy Agency, Paris, France.

430   Krishna, R., Standart, G.L., 1979. Mass and Energy Transfer in Multicomponent Systems. Chem. Eng. Comm., 3,

431   201–276.

432   Krishnamurthy, R., Taylor, R., 1985. A nonequilibrium stage model of multicomponent separation processes.

433   Part I: Model description and method of solution. AIChE J., 31, 449–456.

434 Lee, A.S., Eslick, J.C., Miller, D.C., Kitchin, J.R., 2013. Comparisons of amine solvents for post-combustion CO2

435 capture: A multi-objective analysis approach. Int. J. Greenh. Gas Control, 18, 68–74.

436 Liebenthal, U., Pinto, D.D., Monteiro, J.G. M., Svendsen, H.F., Kather, A., Overall Process Analysis and

437 Optimisation for CO2 Capture from Coal Fired Power Plants based on Phase Change Solvents Forming

438 Two Liquid Phases. Energy Procedia, 2013, 37, 1844-1854.

439 Mac Dowell, N., Llovell, F., Adjiman, C. S., Jackson, G., Galindo, A., 2010. Modeling the Fluid Phase Behavior of

440 Carbon Dioxide in Aqueous Solutions of Monoethanolamine Using Transferable Parameters with the

441 SAFT-VR Approach. Ind. Eng. Chem. Res., 49, 1883–1899.

442 Mac Dowell N, Samsatli NJ, Shah N, 2013. Dynamic modelling and analysis of an amine-based post-combustion

443 CO_2 capture absorption column. International Journal of Greenhouse Gas Control, 12: 247–258.

444 Mangalapally, H.P., Hasse, H., 2011a. Pilot Plant Experiments for Post Combustion Carbon Dioxide Capture by

445 Reactive Absorption with Novel Solvents. Energy Procedia, 4, 1–8.

446 Mangalapally, H.P., Hasse, H., 2011b. Pilot plant study of post-combustion carbon dioxide capture by reactive

447 absorption: Methodology, comparison of different structured packings, and comprehensive results for

448 monoethanolamine. Chem. Eng. Res. Des., 89, 1216–1228.

449 Mangalapally, H.P., Notz, R., Asprion, N., Sieder, G., Garcia, H., Hasse, H., 2012. Pilot plant study of four new

450 solvents for post combustion carbon dioxide capture by reactive absorption and comparison to MEA. Int.

451 J. Greenh. Gas Control, 8, 205–216.

452 McCabe, W., Smith, J., Harriott, P., 2004. Unit Operations of Chemical Engineering, 7th edition, McGraw Hill

453 Chemical Engineering Series.

454 Mores P., Scenna N., Mussati S., 2012. CO2 capture using monoethanolamine (MEA) aqueous solution:

455 Modeling and optimization of the solvent regeneration and CO2 desorption process. Energy, 45, 1042-

456 1058.

457 Moser, P., Schmidt, S., Sieder, G., Garcia, H., Stoffregen, T., 2011a. Performance of MEA in a long-term test at

458 the post-combustion capture pilot plant in Niederaussem. Int. J. Greenh. Gas Control, 5, 620–627.

459 Moser, P., Schmidt, S., Sieder, G., Garcia, H., Stoffregen, T., Stamatov, V., 2011b. The post-combustion capture

460 pilot plant Niederaussem - Results of the first half of the testing programme. Energy Procedia, 4, 1310–

461 1316.

462   Oexmann, J., Kather, A., 2010. Minimising the regeneration heat duty of post-combustion CO2 capture by wet

463   chemical absorption: The misguided focus on low heat of absorption solvents. Int. J. Greenh. Gas Control,

464   4 (1), 36–43.

465   Onda, K., Takeuchi, H., Okumoto, Y., 1968. Mass transfer coefficients between gas and liquid phases in packed

466   columns. Journal of Chemical Engineering of Japan, 1, 56–62.

467   Peters, M.S., Timmerhaus, K.D., West, R.E., 2004. Plant design and economics for chemical engineers, 5th

468   edition, McGraw-Hill Chemical Engineering series.

469   Rabensteiner, M., Kinger, G., Koller, M., Gronaldd, G., Hochenauer, C., 2014. Pilot plant study of

470   ethylenediamine as a solvent for post combustioncarbon dioxide capture and comparison to

471   monoethanolamine. Int. J. Greenh. Gas Control, 27, 1–14.

472   Seader, J.D., Henley, E.J., Roper D. K., 2013. Separation Process Principles, 3rd edition, John Wiley & Sons,

473   Hoboken, N.J.

474   Sharifzadeh M., Thornhill N.F., 2012. Optimal selection of control structures using a steady-state inversely

475   controlled process model. Computers & Chemical Engineering, 38 (5), 126–138.

476   Sharifzadeh, M., Thornhill, N.F., 2013. Integrated design and control using a dynamic inversely controlled

477   process model. Computers & Chemical Engineering, 48, 121–134.

478   Sharifzadeh, M., 2013a. Integration of process design and control: a review, Chemical Engineering Research

479   and Design, 91 (12), 2515–2549.

480   Sharifzadeh, M., 2013b. Implementation of an inversely controlled process model for integrated design and

481   control of an ETBE reactive distillation, Chemical Engineering Science. 92, 21–39.

482   Sharifzadeh, M., Wang, L., Shah, N., 2015. Integrated bio-refineries: CO_2 utilization for maximum biomass

483   conversion. Renewable and Sustainable Energy Reviews, 47, 151–161.

484   Taylor, R., Kooijman, H. A., Hung JS, 1994. A second generation nonequilibrium model for computer simulation

485   of multicomponent separation processes, Comput. Chem. Eng., 18, 205-217.

486   Taylor, R., Krishna, R., 1993. Multicomponent Mass Transfer, John Wiley & Sons, New York.

487   Thee, H., Suryaputradinata, Y. A., Mumford, K. A., Smith K.H., da Silva G., Kentish S.E., Stevens G.W., A kinetic

488   and process modeling study of CO2 capture with MEA-promoted potassium carbonate solutions, Chem.

489   Eng. J., 2012, 210, 271–279.

490   Ulrich, G.D., Vasudevan, P.T., 2006. How to estimate utility costs, Chem. Eng. April, 66–69.

491   Waggoner, R.C., Loud, G.D., 1977. Algorithms for the solution of material balance equations for non-

492   conventional multi-stage operations, Comput. Chem. Eng., 1, 49–56.

493   Wertheim, M.S., 1984. Fluids with highly directional attractive forces. II. Thermodynamic perturbation theory

494   and integral equations. J. Stat. Phys., 35, 35–47.

495   Yang, N., Xu, D.Y., Yu, H., Conway, W., Maeder, M., Feron, P., 2014. Potassium sarcosinate promoted aqueous

496   ammonia solution for post-combustion capture of CO2, Greenhouse Gases-Science And Technology, 4 (4),

497   555-567.

498   Zhang, Y., Chen, H., Chen, C.C., Plaza J.M., Dugas R., Rochelle G.T., 2009. Rate-based process modeling study of

499   CO2 capture with aqueous monoethanolamine solution. Industrial & Engineering Chemistry Research,

500   48(20), 9233-9246.